# Novel Circulating Fluidized-Bed Membrane Reformer Using Carbon Dioxide Sequestration

**Pradeep Prasad* and Said S. E. H. Elnashaie**

*Chemical Engineering Department, Auburn University, Auburn, Alabama 36849*

A novel circulating fluidized-bed membrane reactor employing a reactor−regenerator type of configuration is proposed for hydrogen production by the steam reforming of natural gas. The reactor section of this configuration is investigated. $CO_2$ sequestration using the $CO_2$−lime reaction is utilized to assist/replace the hydrogen permselective membranes for "breaking" the thermodynamic equilibrium of the reversible reforming reactions. Cases with and without CaO and hydrogen permselective membranes are considered and compared. A slip velocity factor is incorporated to investigate the effect of CaO particle size/residence time on the conversion of lime and the overall performance of the reformer.

## Introduction

Steam reforming is the most efficient means of producing hydrogen/syngas from methane, and fixed beds are currently the dominant reformer configuration in industry (first-generation reformers[1]). These classical industrial reformers consist of hundreds of parallel catalyst tubes surrounded by a very large top or side-fired furnace supplying the necessary heat for the highly endothermic reforming reactions. Relatively large Ni-based catalyst particles are used to avoid excessive pressure drop along the reformer tubes. This design suffers from a number of limitations that decrease the efficiency and lead to the huge size of the equipment. Because of the large size of the catalyst pellets, intraparticle diffusion limitations reduce the effectiveness factors to values as low as $10^{-2}$−$10^{-3}$.[1] The reversible nature of the reactions limits the conversion to that of the thermodynamic equilibrium and necessitates the use of elevated temperatures to achieve acceptable levels of conversion. Also, carbon formation increases with an increase in the temperature and leads to deactivation of the catalyst, thus necessitating the use of a high steam-to-hydrocarbon ratio.

Elnashaie and Adris[2] were the first to propose the use of a bubbling fluidized-bed steam reformer (second-generation reformer, SGR) using a powdered catalyst to overcome the diffusional limitations of the catalyst pellets and thus increase the effectiveness factor 100−1000-fold. The SGR underwent further remarkable enhancements in performance, by the use of composite hydrogen permselective membranes to "break" the thermodynamic equilibrium barrier in order to push the reactions toward higher conversions, even at low temperatures.[3] Adris[4] and Adris et al.[5] further studied, validated, and patented[6] the fluidized-bed membrane reformer (FBMR) after building a pilot plant and undertaking experimental and modeling studies of the system. The FBMR configuration, although very efficient, still suffers from some limitations with regard to the flow rate that can be used in a bubbling fluidized-bed, thereby preventing the full exploitation of the increase in the catalyst effectiveness factor. Furthermore, it is not the most suitable configuration for higher hydrocarbons because it does not have the best provision for handling the excessive carbon formation associated with higher hydrocarbons and/or operation at low steam-to-hydrocarbon ratios.

Recently, a more efficient and flexible circulating fluidized-bed configuration has been proposed,[7,8] and the use of hydrogen permselective composite membranes[9−14] was studied for breaking the thermodynamic equilibrium barrier. The present paper presents a further investigation of the configuration where, in addition to the hydrogen permselective membranes, lime is used as an absorbent for the carbon dioxide produced, thus promoting the reforming reactions. The circulating fluidized-bed configuration is well suited for the use of CaO because the product $CaCO_3$ can be regenerated and fed back to the riser reformer.

Both the hydrogen-permeable membranes and the lime−$CO_2$ reaction utilize the same principle of combining reaction and separation steps via removal of one of the products of the reaction from the reaction mixture to promote the reversible reforming reactions. Silaban and Harrison[15] studied the reversible reaction between CaO and $CO_2$ for application in the control of $CO_2$ emissions from power generation processes. Han and Harrison[16] utilized this concept to carry out the shift conversion reaction without the presence of the shift catalyst. Balasubramanian et al.[17] proposed a single-step process for obtaining 95% pure hydrogen directly from steam reforming of methane, eliminating the need for a separate shift converter. For efficient use of the sorbent in a process based on $CO_2$ separation, it is important for the sorbent to be able to retain its activity through several cycles between the oxide and the carbonate stages. Han and Harrison[18] reported a better multicycle performance of dolomite as compared to limestone because of the structural differences between the two. Hufton et al.[19] and Waldron et al.[20] have reported a proprietary potassium carbonate promoted, hydrotalcite-based sorbent, which has better properties. However, reaction rate data are not available in the open literature for the proprietary sorbent. Multicycle tests for dolomite reported by Han and Harrison[18] showed only moderate deterioration in the acceptor performance. However, a greater loss of activity is

* To whom correspondence should be addressed. Tel.: 1-334-8442051. Fax: 1-334-8442063. E-mail: prasa01@auburn.edu.

10.1021/ie030524i CCC: $27.50 
Published on Web 12/18/2003

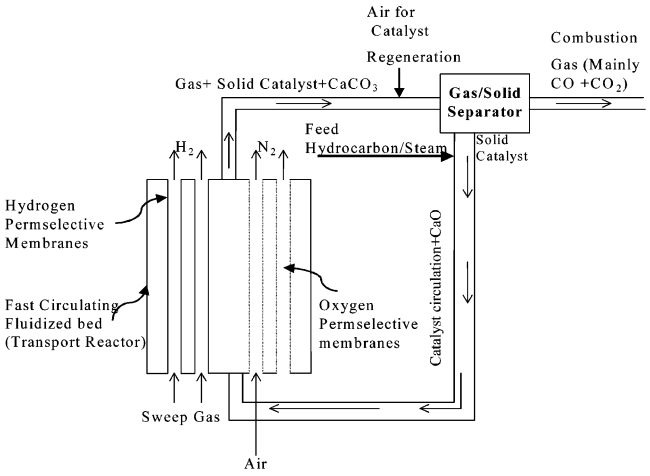


**Figure 1.** Schematic diagram of the proposed novel configuration.

reported for CaO by Abanades,[21] who incorporated a fresh feed of the sorbent to make up for the lost activity.

## Main Features of the Present Novel Configuration (Third-Generation Reformer, TGR)

A short description of the proposed circulating fluidized-bed configuration is given here (Figure 1). A more detailed description of the configuration is given by Prasad and Elnashaie[7] and Chen et al.[8] The reformer part of the configuration is a riser reactor utilizing powdered catalyst particles. The thermodynamic equilibrium limitations of the reforming reactions are broken using hydrogen permselective membranes[9−14] and/or a $CO_2$ acceptor such as CaO.[15−21] The reaction between lime and $CO_2$, being exothermic, supplies a part of the heat necessary for the endothermic reforming reactions. The novel design is quite versatile in terms of the feedstocks that may be used because of the provision for handling excessive carbon formation. This is because the problem of deactivation of the catalyst by coke deposition[22,23] can be addressed by burning off the carbon in a regenerator before recirculating the hot regenerated catalyst to the reformer. The regeneration may be done in a transport reactor or in a bubbling fluidized bed depending on the amount of carbon formed and the residence time required for its combustion. The high temperature of the regenerator helps to reconvert the calcium carbonate to calcium oxide in spite of the $CO_2$-rich atmosphere in the regenerator because of the increased equilibrium pressure of carbon dioxide at higher temperatures. Preliminary investigations of this aspect of the configuration are promising. Studies of the complete configuration along with the regeneration cycle and its effects on the overall design and modes of operation will be presented in a subsequent paper.

## The Model

The present paper considers the riser reformer part of the novel circulating fluidized-bed configuration, with steam-reforming reactions taking place in the presence of suitable permselective membranes to remove the product hydrogen and CaO to remove the product carbon dioxide. Different parameters for measuring the efficiency of the reformer are employed.

**Rate Equations. (a) Methane Steam Reforming.** The nonmonotonic rate expressions proposed by Xu and Froment[24] for a Ni-based catalyst and analyzed in some detail by Elnashaie et al.[25] are used in the present investigation. The three main reactions are given below. The corresponding rate equations and kinetic parameters are available in the work by Xu and Froment[24] and in the work by Elnashaie and Elshishini.[1] Methane steam reforming is highly endothermic while the shift reaction is mildly exothermic, as shown in eqs 1−3.

$$CH_4 + H_2O \rightleftharpoons CO + 3H_2 \qquad (\Delta H° = 206\ \text{kJ·mol}^{-1}) \tag{1}$$

$$CO + H_2O \rightleftharpoons CO_2 + H_2 \qquad (\Delta H° = -41\ \text{kJ·mol}^{-1}) \tag{2}$$

$$CH_4 + 2H_2O \rightleftharpoons CO_2 + 4H_2 \qquad (\Delta H° = 165\ \text{kJ·mol}^{-1}) \tag{3}$$

**(b) Carbon Dioxide Sequestration.** The reaction between $CO_2$ and the absorbent (e.g., lime, dolomite, etc.) shows a faster reaction-controlled initial period followed by a much slower second stage, which is controlled by the diffusion of $CO_2$ through the product layer.[26,27] In this paper, the reaction is assumed to be in the reaction control regime because of the relatively short contact time in the riser reformer and because of the relatively low levels of CaO conversion. The corresponding kinetic expression and constants have been extracted from the work of Bhatia and Perlmutter.[26] They have reported that the rate constant has zero activation energy for the temperature range 823−998 K. The reaction of carbon dioxide with CaO not only has a positive effect on the reaction equilibrium but also releases some heat because of its exothermic nature.

$$CaO + CO_2 \rightleftharpoons CaCO_3 \qquad (\Delta H° = -178\ \text{kJ·mol}^{-1}) \tag{4}$$

$$r_4 = k_x(1 - X_{CaO})\sqrt{1 - \phi \ln(1 - X_{CaO})}(C_{CO_2} - C_{CO_2,e}) \tag{5}$$

**(c) Assumptions.** The following simplifying assumptions are included in the model derivation:

(1) All parts of the system are at steady state.

(2) The reformer gas, catalyst, and $CO_2$ absorbent are flowing in plug flow through the reformer at the same speed (this assumption is relaxed later in the paper with regards to the $CO_2$ absorbent).

(3) Negligible axial mixing and complete radial mixing.

(4) The volume fraction of total solid remains constant along the length of the reactor.

(5) The membranes are completely permselective, in thermal equilibrium with the reformer gases and in cocurrent mode.

(6) Pure absorbent (CaO) is fed to the reformer.

(7) Ideal gas laws are applicable.

(8) Heat losses are negligible.

**Model Equations.** The design equations involve seven components, viz., $CH_4$, $H_2O$, CO, $CO_2$, $H_2$, CaO, and $CaCO_3$. Thus, there are seven mass balance equations and one energy balance equation for the reactor side and one mass balance for the membrane side. The heat balance equation considers the heat capacities of the flowing gases as well as the solids (CaO, $CaCO_3$,

and catalyst). The partial pressures involved are calculated using the ideal gas relation.

$$\frac{dF_i}{dl} = \rho_{cat.}(1-\alpha)(1-\epsilon)A_r R_i - mJ_i \qquad i = CH_4, H_2O, CO, H_2 \quad (6)$$

$$\frac{dF_{CO_2}}{dl} = \rho_{cat.}(1-\alpha)(1-\epsilon)A_r(r_2+r_3) - \rho'_{CaO}\alpha(1-\epsilon)A_r r_4 \quad (7)$$

$$\frac{dF_i}{dl} = \rho'_{CaO}\alpha(1-\epsilon)A_r r_4 \qquad i = CaO, CaCO_3 \quad (8)$$

$$\sum_i F_i \frac{d(H_i)}{dl} = \rho_{cat.}(1-\alpha)(1-\epsilon)A_r \sum_{j=1}^{3} r_j(-\Delta H_j) + \rho'_{CaO}\alpha(1-\epsilon)A_r r_4(-\Delta H_4) + Q \quad (9)$$

In eq 6, $R_i = 0$ for the hydrogen membrane-side-equation mass balance and $J_i = 0$ for all components in the reactor-side equations except hydrogen, for which $J_i$ is the corresponding molar permeation term depending on the type of membrane used. The value of $m$ is 1 in the reactor-side equation and $-1$ in the membrane-side equation for hydrogen. For a supported Pd membrane tube, the hydrogen permeation term[9] is given below. Values of parameters extracted from Nam and Lee[14] are used in the present investigation.

$$J_{H_2} = Q_{H_2}\left(\frac{\pi d_m n_t}{\delta_{H_2}}\right)\exp\left(\frac{-E_{H_2}}{RT}\right)(p_{H_2,r}{}^n - p_{H_2,m}{}^n) \quad (10)$$

$\alpha$ is the volumetric ratio of CaO to the total solids (CaO + catalyst) in the reactor. It is calculated from the feed mass ratio of CaO to catalyst ($\gamma$) and slip factor ($\psi$) using eq 11. The slip factor ($\psi$) is the ratio between the CaO particle velocity ($v_p$) and the actual gas velocity ($U_0/\epsilon$). The initial part of this paper assumes a slip factor of 1, which is relaxed in the section where the effect of the CaO particle size is studied. Patience et al.[28] have proposed a correlation based on the Froude number for calculating the slip factor in the fully developed region of fast fluidized and pneumatic transport risers. For calculating the slip factor using the particle Froude number ($Fr_t$), the terminal velocity of the particle is required and is calculated from the correlation for dimensionless terminal velocity proposed by Haider and Levenspiel.[29]

$$\alpha = \frac{\gamma\psi\rho_{cat.}}{\rho_{CaO} + \gamma\psi\rho_{cat.}} \quad (11)$$

$$\psi = \left(\frac{U_0}{\epsilon v_p}\right) = 1 + \frac{5.6}{Fr} + 0.47 Fr_t{}^{0.41} \quad (12)$$

$$u_t^* = \left(\frac{18}{d_p^{*2}} + \frac{0.591}{d_p^{*1/2}}\right)^{-1} \quad (13)$$

where

$$u_t^* = u_t\left[\frac{\rho_f{}^2}{g\mu(\rho_{CaO} - \rho_f)}\right]^{1/3} \quad (14)$$

$$d_p^* = d_p\left[\frac{g\rho_f(\rho_{CaO} - \rho_f)}{\mu^2}\right]^{1/3} \quad (15)$$

In all of the results of the present investigation, the generalized map of gas/solid contacting reported by Kunii and Levenspiel[30] is used to ensure that the reactor is in either the fast fluidization or the pneumatic transport regime.

**Solution of the Model Equations.** The set of nonlinear initial value differential equations is accurately solved using the IVPAG subroutine from the IMSL libraries. The set of differential equations is solved using the initial conditions of the methane feed per tube (3.953 kmol of $CH_4$ per hour with a steam-to-methane ratio of 3.561) of an industrial fixed-bed reformer described by Elnashaie and Elshishini.[1] A nonzero amount of hydrogen (0.04 kmol·h$^{-1}$ in the present case) is required in the feed in order to avoid division by zero in the steam-reforming reaction rates. The following additional data are used unless otherwise stated: the solid fraction in the reactor ($1 - \epsilon$) is 0.1, the cross-sectional area ($A_c$) of the reactor available for flow of the reactants is 75.12 cm$^2$, the diameter of the hydrogen membrane tubes ($d_m$) is 5 mm, the number of hydrogen-permeable tubes is 5, the pressure on the hydrogen-permeable membrane side is 1 atm, and the flow rate of the inert sweep gas is 1 kmol·h$^{-1}$. The total hydrogen yield is calculated as the total amount of hydrogen produced per mole of methane fed.

$$Y_{H_2} = \frac{F_{H_2}^m + F_{H_2} - F_{H_2}^0}{F_{CH_4}^0} \quad (16)$$

## Results and Discussion

Figure 2 shows the effect of CaO and hydrogen permselective membranes. The reaction reaches the equilibrium methane conversion (58.3%) in the absence of both CaO and hydrogen permselective membranes with an exit temperature of 895 K. Both CaO and hydrogen permselective membranes have a positive effect on methane conversion. The exothermic reaction of CaO and $CO_2$ helps to increase the temperature, whereas when the hydrogen permselective membranes are used, the higher extent of reaction causes a further drop in the temperature. Consequently, for the cases compared here, the conversion with CaO is slightly higher (~1.8%) than the conversion with the membranes. When CaO is used together with the hydrogen membranes, the conversion is about 17.4% higher than the case when only CaO is used, 19.5% higher than the case when only hydrogen permselective membranes are used, and 46.1% higher than the case when neither is used.

Figure 3a shows the effect of the feed temperature on CaO and membrane-assisted breaking of the thermodynamic equilibrium barrier. Above 950 K, when a combination of the two techniques is used, the system very closely approaches the maximum theoretical value for hydrogen yield of 4. The yield with membranes becomes greater than the yield obtained with CaO above

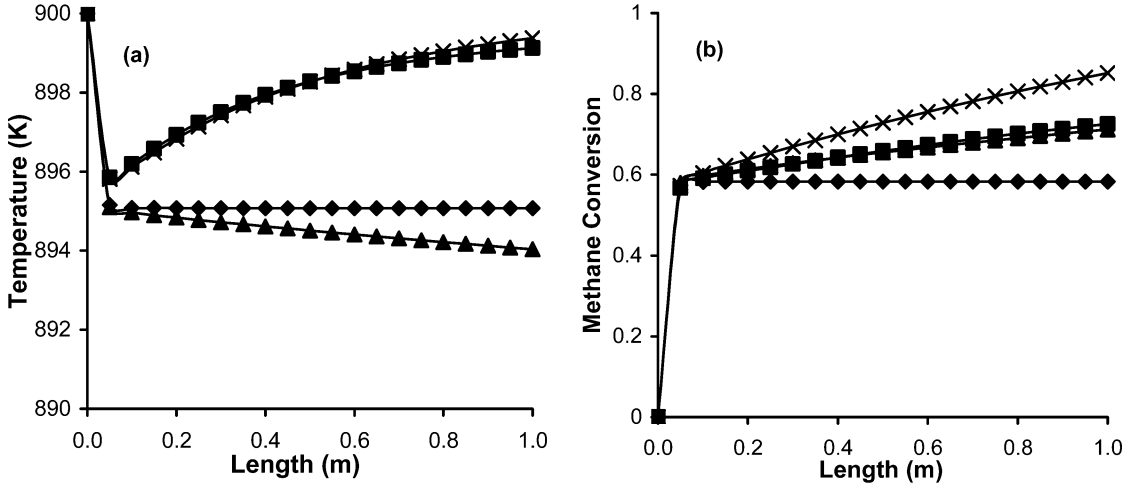


**Figure 2.** Effect of the techniques to break the equilibrium ($T_f$ = 900 K, $P$ = 5 atm, and $\gamma$ = 0.5): (◆) without CaO and without $H_2$ permselective membranes; (■) with CaO and without $H_2$ permselective membranes; (▲) without CaO and with $H_2$ permselective membranes; (×) with CaO and $H_2$ permselective membranes.

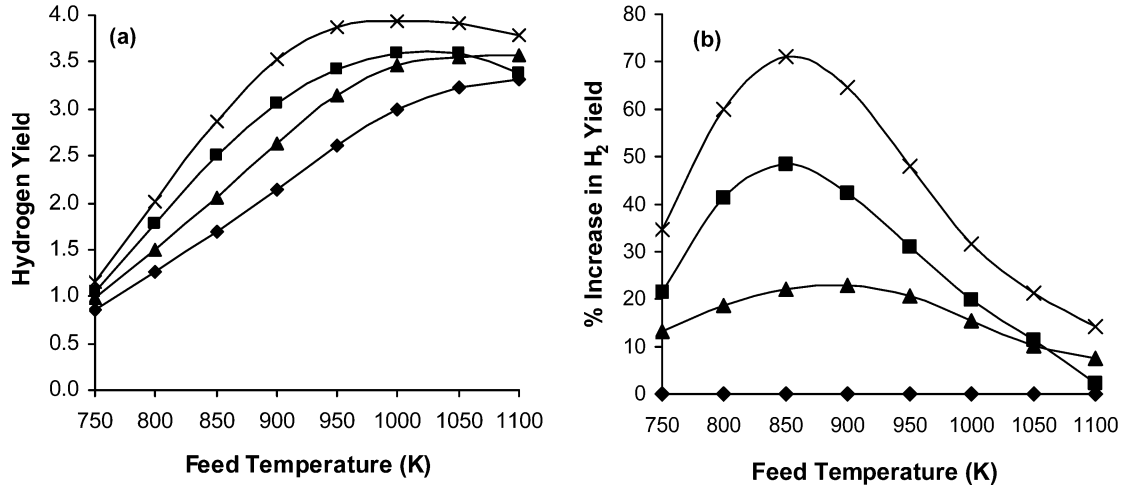


**Figure 3.** Effect of the feed temperature ($P$ = 5 atm and $\gamma$ = 1.0): (◆) without CaO and without $H_2$ permselective membranes; (■) with CaO and without $H_2$ permselective membranes; (▲) without CaO and with $H_2$ permselective membranes; (×) with CaO and $H_2$ permselective membranes.

1050 K because of the increase in equilibrium $CO_2$ pressure ($C_{CO_2,e}$) with temperature. Figure 3b compares the percentage increase in the hydrogen yield over that for the case with neither CaO nor membranes and shows a maximum at 850 K, where the case with CaO and no membranes shows about twice the increase in percentage of hydrogen yield than the case with membranes and without CaO. Again this is due to the exothermic reaction between lime and $CO_2$. A combination of CaO and membranes gives the largest increase in the hydrogen yield (68.9%). As the temperature increases, the equilibrium yield itself increases; hence, in all of the cases we see a decrease in the percentage of hydrogen yield improvement with temperature.

The reforming reaction involves an increase in the number of moles, and hence the equilibrium hydrogen yield decreases with increasing pressure. However, the lime−$CO_2$ reaction depends on the difference in the $CO_2$ concentration in the reactor and the equilibrium $CO_2$ concentration (which is a function of temperature). The case with CaO, therefore, shows a gradual decrease in the yield with pressure, but this is less drastic than the case with neither CaO nor membranes probably because of the lower partial pressure of $CO_2$ as compared to $H_2$. Hydrogen permeation through the membranes also depends on the hydrogen partial pressure difference between the reactor and membrane sides. Hence, higher pressures are favorable to both the lime−$CO_2$ reaction and hydrogen permeation. Because of these contradicting factors, the reformer with membranes shows a nonmonotonic dependence of the hydrogen yield on the reactor pressure, where there is first a decrease and then an increase in the hydrogen yield (see Figure 4). The hydrogen yield when using membranes is lower than that when using CaO until a pressure of about 12 atm, above which the membrane reformer gives a higher yield than the CaO reformer because of the increase in pressure difference between the reactor and membrane sides.

The use of an increased amount of CaO results in a greater amount of $CO_2$ reacting with CaO, and this helps the reforming reaction. Also the heat released in the $CO_2$−lime reaction is useful for the endothermic reforming reactions. However, beyond a certain point, increasing the amount of CaO has a diluting effect both with respect to the heat released and with respect to the rate of the reforming reaction. This leads to a plateau in the hydrogen yield, as seen in Figure 5a, or in some cases a maximum in yield, as seen in Figure 5b. The optimum ratio of catalyst ($\gamma$) thus depends on

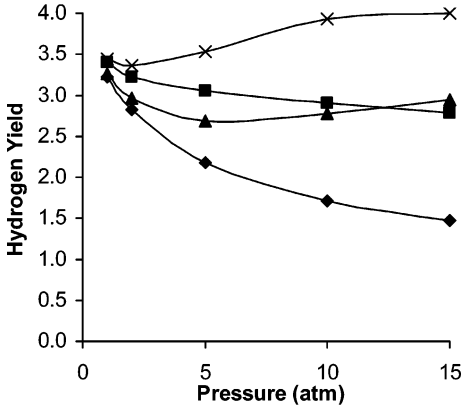


**Figure 4.** Effect of the pressure ($T_f$ = 900 K and $\gamma$ = 1.0): (◆) without CaO and without $H_2$ permselective membranes; (■) with CaO and without $H_2$ permselective membranes; (▲) without CaO and with $H_2$ permselective membranes; (×) with CaO and $H_2$ permselective membranes.

the operating conditions of the reactor. In Figure 5b, the maximum hydrogen yield increases with the number of membranes, but the optimum value of $\gamma \sim 0.8$ does not seem to be affected strongly by the presence of membranes.

In all of the previous results for a wide range of operating conditions, it is observed that the use of CaO alone does not give complete conversion of methane. However, when the hydrogen-permeable membranes are used in conjunction with CaO, it is possible to get complete conversion of methane and the yield of hydrogen almost equal to the maximum value of 4. As seen in Figure 6, increasing the number of membranes for the $\gamma = 0$ (no CaO case) increases the hydrogen yield, but the yield versus number of membranes curve tends to flatten out. Likewise, when no membranes are present, increasing the amount of CaO increases the hydrogen yield, but the rate of increase progressively decreases and, at $\gamma = 1.0$, the yield is still well below the theoretical maximum value of 4. On the other hand, when CaO is used along with membranes, the two techniques of "breaking" the thermodynamic equilibrium barrier complement each other, and it is possible to attain the same or higher hydrogen yield using a lower number of membranes along with CaO than when using membranes alone. In the case shown in Figure 6, the maximum theoretical value for hydrogen yield using methane (i.e., 4.0) is approached using about 15 membranes in the presence of CaO. The membrane requirement increases with a decrease in CaO and the hydrogen yield value of 4 is not obtained even with 50 membrane tubes when CaO is not used ($\gamma = 0$).

Table 1 shows the conversion of CaO for a variety of operating conditions. As with the hydrogen yield, the conversion of CaO increases with the feed temperature and pressure and in the presence of membranes. At a high CaO-to-catalyst ratio ($\gamma$), the effect of CaO in breaking the equilibrium is greater, but only a small fraction of the CaO is utilized. At a lower value of $\gamma$, the methane conversion and the hydrogen yield are less, but the CaO conversion increases. Still the conversion of CaO is below 10% for all but two cases in Table 1. Case 9 shows the highest CaO conversion in Table 1 because it has a smaller CaO-to-catalyst ratio than case 8 while still obtaining a high methane conversion because of the high pressure in the presence of membranes. Low CaO conversion is actually a common observation made in all of the cases discussed thus far. This is due to the slow rate of the lime−$CO_2$ reaction as compared to the reforming reactions. The amount of CaO required ($\gamma$) is consequently several times the feed methane even though the lime−$CO_2$ reaction has 1:1 stoichiometry.

**Effect of the CaO Particle Size.** Increasing the particle size for CaO increases the slip between the gases and CaO particles and increases the CaO residence time. A binary solid size distribution was investigated, where the catalyst has a very small diameter (to obtain a high effectiveness factor) but the CaO particles are larger. The no-slip assumption used thus far is relaxed for CaO in order to accommodate the effect of the CaO particle velocity ($v_p$). The molar flow rates of CaO and $CaCO_3$ can be written as below, where $C_{CaO}$ and $C_{CaCO_3}$ are the moles of CaO and $CaCO_3$ per unit volume of solid (CaO + $CaCO_3$), respectively.

$$F_i = A_r(1-\epsilon)\psi\left(\frac{U_0}{\epsilon}\right)\alpha C_i \qquad (i = \text{CaO and } CaCO_3) \tag{17}$$

The balances for CaO and $CaCO_3$ in eq 8 can now be modified to include the effect of the particle velocity and written as shown below. The equation assumes a constant particle velocity (which in this case was calculated using the slip factor at the inlet). This simplifying assumption can be expected not to alter the nature of the results qualitatively. The feed to the

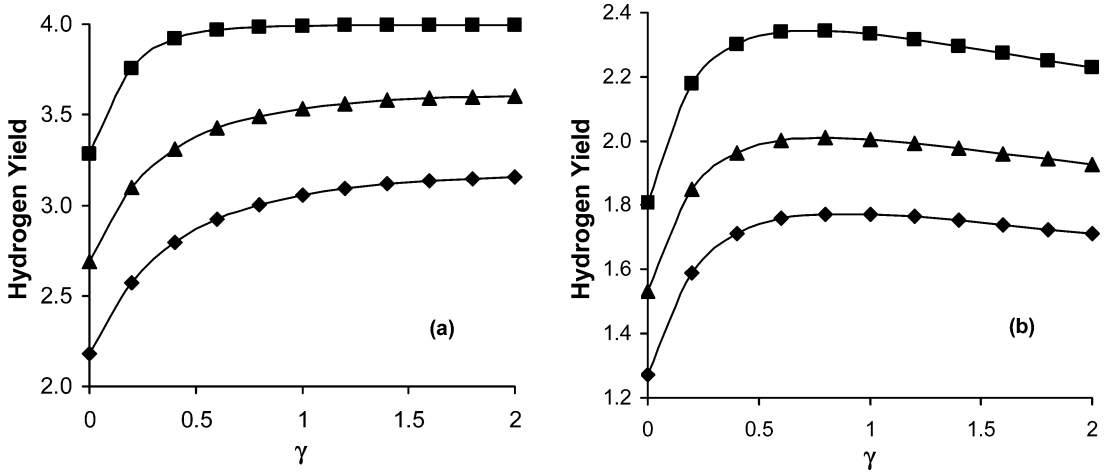


**Figure 5.** Effect of the CaO-to-catalyst ratio: (◆) $n_t$ = 0; (▲) $n_t$ = 5; (■) $n_t$ = 15. (a) $T_f$ = 900 K; $P$ = 5 atm. (b) $T_f$ = 800 K; $P$ = 5 atm.

**Table 1. CaO Conversion for Different Operating Conditions**

| no. | $T_f$ (K) | $P$ (atm) | $\gamma$ | $n_t$ | $X_{CH_4}$ | % increase in $X_{CH_4}$[a] | $Y_{H_2}$ | % increase in $Y_{H_2}$[a] | $X_{CaO}$ | $F^0_{CaO}$ (kmol·h$^{-1}$) |
|---|---|---|---|---|---|---|---|---|---|---|
| 1 | 900 | 5 | 1 | 0 | 0.7637 | 31.27 | 3.0319 | 39.42 | 0.0039 | 713.06 |
| 2 | 900 | 10 | 1 | 0 | 0.7221 | 60.36 | 2.8804 | 68.45 | 0.0078 | 356.53 |
| 3 | 900 | 10 | 0.1 | 0 | 0.5412 | 20.19 | 2.1249 | 24.27 | 0.0275 | 56.19 |
| 4 | 850 | 5 | 0.1 | 5 | 0.5895 | 32.89 | 2.3114 | 35.79 | 0.0117 | 106.13 |
| 5 | 850 | 10 | 0.1 | 5 | 0.6347 | 86.90 | 2.5185 | 91.24 | 0.0356 | 53.07 |
| 6 | 900 | 5 | 0.1 | 5 | 0.7473 | 28.45 | 2.8902 | 32.90 | 0.0126 | 112.38 |
| 7 | 900 | 10 | 0.1 | 5 | 0.8186 | 81.79 | 3.2341 | 89.14 | 0.0425 | 56.19 |
| 8 | 900 | 20 | 0.1 | 5 | 0.9921 | 190.6 | 3.9636 | 201.76 | 0.1315 | 28.09 |
| 9 | 900 | 20 | 0.04 | 5 | 0.9127 | 167.34 | 3.6256 | 176.03 | 0.2237 | 11.69 |

[a] Increase over the case with no CaO or membranes.

**Table 2. Effect of the CaO Particle Size ($n_t = 5$)**

| $d_p$ ($\mu$m) | $\psi$ | $X_{CH_4}$ | % increase in $X_{CH_4}$[a] | $Y_{H_2}$ | % increase in $Y_{H_2}$[a] | $X_{CaO}$ | % increase in $X_{CaO}$[a] | $F^0_{CaO}$ (kmol·h$^{-1}$) |
|---|---|---|---|---|---|---|---|---|
| | | | $T_f = 900$ K, $P = 5$ atm, and $\gamma = 0.1$ | | | | | |
| 20 | 1.2471 | 0.7559 | 1.15 | 2.9345 | 1.53 | 0.0148 | 17.46 | 110.6265 |
| 100 | 1.5492 | 0.7662 | 2.53 | 2.9857 | 3.30 | 0.0171 | 35.71 | 108.5606 |
| 500 | 2.2732 | 0.7879 | 5.43 | 3.0905 | 6.93 | 0.0216 | 71.43 | 103.9097 |
| 1000 | 2.6247 | 0.7971 | 6.67 | 3.1333 | 8.41 | 0.0234 | 85.71 | 101.7924 |
| 2000 | 2.9515 | 0.8048 | 7.69 | 3.1690 | 9.65 | 0.0250 | 98.41 | 99.8997 |
| | | | $T_f = 900$ K, $P = 10$ atm, and $\gamma = 0.1$ | | | | | |
| 20 | 1.3768 | 0.8457 | 3.31 | 3.3523 | 3.65 | 0.0497 | 16.94 | 54.8651 |
| 100 | 1.6712 | 0.8628 | 5.40 | 3.4263 | 5.94 | 0.0541 | 27.29 | 53.8740 |
| 500 | 2.3049 | 0.8910 | 8.84 | 3.5460 | 9.64 | 0.0613 | 44.24 | 51.8576 |
| 1000 | 2.5884 | 0.9006 | 10.02 | 3.5868 | 10.91 | 0.0640 | 50.59 | 51.0034 |
| 2000 | 2.8554 | 0.9085 | 10.98 | 3.6198 | 11.93 | 0.0662 | 55.76 | 50.2244 |
| | | | $T_f = 900$ K, $P = 20$ atm, and $\gamma = 0.04$ | | | | | |
| 20 | 1.6362 | 0.9633 | 5.54 | 3.8395 | 5.90 | 0.2838 | 26.87 | 11.4917 |
| 100 | 1.9206 | 0.9763 | 6.97 | 3.8950 | 7.43 | 0.3011 | 34.60 | 11.4068 |
| 500 | 2.4646 | 0.9912 | 8.60 | 3.9591 | 9.20 | 0.3253 | 45.42 | 11.2478 |
| 1000 | 2.6932 | 0.9945 | 8.96 | 3.9736 | 9.60 | 0.3329 | 48.82 | 11.1823 |
| 2000 | 2.9135 | 0.9965 | 9.18 | 3.9830 | 9.86 | 0.3392 | 51.63 | 11.1199 |

[a] Increase over the corresponding no-slip case from Table 1.

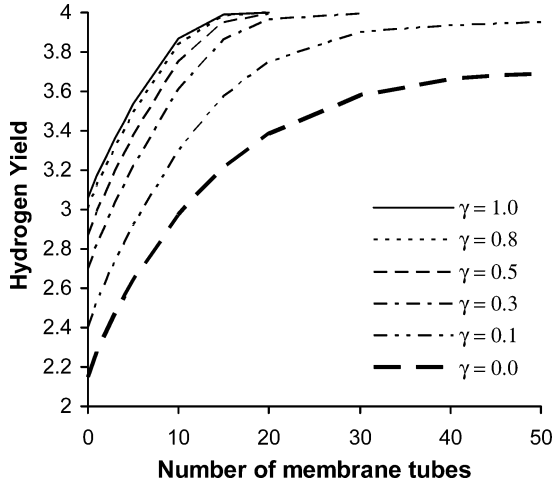


**Figure 6.** Additive effect of the CaO and hydrogen permselective membranes ($T_f = 900$ K and $P = 5$ atm).

reactor (initial condition) is considered to be pure CaO so that $C_{CaO}$ (at $l = 0$) is equal to $\rho'_{CaO}$.

$$\frac{dC_i}{dl} = \frac{\rho'_{CaO} r_4}{v_p} \qquad (i = \text{CaO and } CaCO_3) \qquad (18)$$

As seen in Table 2, the relaxation of the no-slip assumption and the increase in the CaO particle size results in higher CaO conversion than the corresponding case in Table 1 and further increases with the particle size. For a small particle size, the slip factor ($\psi$) is relatively close to 1 and the increase in the methane conversion and the hydrogen yield over the no-slip assumption results of Table 1 are small. As the particle size increases, the residence time of CaO in the reformer increases and hence the amount of CaO reacted also increases. The increase in the particle size also enhances the methane conversion and the hydrogen yield. Increasing the particle size to about 2 mm increases the hydrogen yield by up to about 12% with respect to the no-slip case. The efficiency of the reformer can be expected to increase with the CaO particle size until we reach a hydrodynamic limitation when the gas velocity becomes equal to or lower than the terminal velocity.

## Conclusion

A circulating fluidized bed was proposed for producing hydrogen using the steam reforming of methane. Modeling investigations were carried out on the fast fluidized membrane reformer part of the circulating fluidized-bed configuration to show the effect of using CaO to assist in breaking of the thermodynamic equilibrium using carbon dioxide sequestration. For some cases, e.g., $T_f = 800$ K and $P = 5$ atm, there is an optimum ratio of CaO to catalyst, and higher values than the optimum can result in a decrease in the hydrogen yield. The use of hydrogen permselective membranes along with CaO was studied, and it was found that complete conversion of methane can be attained with a high yield of hydrogen (up to the theoretical limit of 4) when these two complementary techniques are used together. The effect of the CaO particle size was investigated by

relaxing the no-slip assumption in the reactor model equations. The hydrogen yield, as well as the methane and CaO conversion, increases with an increase of the slip factor. This suggests that the combined use of hydrogen permselective membranes and $CO_2$ sequestration with a binary catalyst/$CO_2$ absorbent particle size can lead to a very efficient circulating fluidized-bed reformer.

## Acknowledgment

This research was supported by Auburn University through Grant 2-12085.

## Notation

$A_r$ = area of cross section of the reactor ($m^2$)
$C_{CO_2}$, $C_{CO_2,e}$ = concentration of $CO_2$ in the reactor, equilibrium concentration of $CO_2$ ($kmol \cdot m^{-3}$)
$d_p$ = diameter of the catalyst particle (m)
$d_p^*$ = dimensionless measure of the particle diameter
$D_t$ = diameter of the reactor (m)
$E_{H_2}$ = apparent activation energy of the composite palladium membrane ($kJ \cdot mol^{-1}$)
$F_i$ = molar flow rate of species $i$ ($kmol \cdot h^{-1}$)
$F_i^0$ = molar feed flow rate of species $i$ ($kmol \cdot h^{-1}$)
$Fr$ = Froude number [$=U_0/(gD_t)^{0.5}$]
$Fr_t$ = particle Froude number [$=u_t/(gD_t)^{0.5}$]
$g$ = acceleration due to gravity [$=9.8\ m \cdot s^{-2}$]
$\Delta H_j$ = heat of reaction for reaction $j$ ($kJ \cdot mol^{-1}$)
$H_i$ = molar enthalpy of species $i$ ($kJ \cdot mol^{-1}$)
$J_{H_2}$ = rate of removal of hydrogen ($kmol \cdot h^{-1} \cdot m^{-1}$)
$k_x$ = rate constant for the CaO carbonation reaction ($m^{-3} \cdot kmol^{-1} \cdot h^{-1}$)
$l$ = distance along the reactor (m)
$n$ = exponent for the partial pressure in the hydrogen permeation term
$n_t$ = number of membrane tubes
$p_{H_2}$, $p_{H_2,m}$ = $H_2$ partial pressure on the reaction and membrane side, respectively (kPa)
$Q_{H_2}$ = preexponential factor ($kJ \cdot m^{-1} \cdot h^{-1} \cdot kPa^{-n}$)
$Q$ = rate of heat input ($kJ \cdot h^{-1} \cdot m^{-1}$)
$r_j$ = rate of reaction $j$ [$kmol \cdot h^{-1} \cdot (kg\ of\ catalyst)^{-1}$ or $h^{-1}$]
$R$ = gas constant ($=8.314\ kJ \cdot kmol^{-1} \cdot K^{-1}$)
$R_i$ = rate of generation of species $i$ [$kmol \cdot h^{-1} \cdot (kg\ of\ catalyst)^{-1}$]
$T$ = temperature (K)
$U_0$ = superficial velocity ($m \cdot s^{-1}$)
$u_t^*$ = dimensionless particle terminal velocity
$v_p$ = CaO particle velocity ($m \cdot s^{-1}$)
$X_{CH_4}$, $X_{CaO}$ = conversion of methane and CaO, respectively
$Y_{H_2}$ = yield of hydrogen

*Greek Letters*

$\alpha$ = $m^3$ of CaO per $m^3$ of total solids at feed
$\gamma$ = (mass of CaO/mass of catalyst) in feed
$\delta$ = thickness of the palladium membrane (m)
$\epsilon$ = void fraction
$\rho_f$ = density of reaction gases ($kg \cdot m^{-3}$)
$\rho_{cat.}$ = density of the catalyst ($kg \cdot m^{-3}$)
$\rho_{CaO}$ = density of CaO ($kg \cdot m^{-3}$)
$\rho'_{CaO}$ = molar density of CaO ($kmol \cdot m^{-3}$)
$\mu$ = viscosity ($kg \cdot m^{-1} \cdot s^{-1}$)
$\psi$ = slip factor

## Literature Cited

(1) Elnashaie, S. S. E. H.; Elshishini, S. S. *Modelling, simulation and optimization of industrial fixed bed catalytic reactors*; Gordon and Breach Science Publishers: London, U.K., 1993.

(2) Elnashaie, S. S. E. H.; Adris, A. M. In *Proceedings of the VI International Fluidization Conference*; Grace, J., Shemilt, L. W., Bergougnou, M. M., Eds.; AIChE Publication: Banff, Canada, 1989; p 319.

(3) Adris, A. M.; Elnashaie, S. S. E. H.; Hughes, R. A Fluidized Bed Membrane Reactor for the Steam Reforming of Methane. *Can. J. Chem. Eng.* **1991**, *69*, 1061.

(4) Adris, A. M. A fluidized bed membrane reactor for steam reforming: experimental verification and model validation. Ph.D. Thesis, University of British Columbia, British Columbia, Canada, 1994.

(5) Adris, A. M.; Lim, C. J.; Grace, J. R. The Fluidized Bed Membrane Reactor for Steam Methane Reforming: Model Verification and Parametric Study. *Chem. Eng. Sci.* **1997**, *52*, 1069.

(6) Adris, A. M.; Grace, J. R.; Lim, C. J.; Elnashaie, S. S. E. H. Fluidized Bed Reaction System for Steam/Hydrocarbon Reforming to Produce Hydrogen. U.S. Patent 5,326,550, 1994.

(7) Prasad, P.; Elnashaie, S. S. E. H. Novel Circulating Fluidized-Bed Membrane Reformer for the Efficient production of Ultraclean Fuels from Hydrocarbons. *Ind. Eng. Chem. Res.* **2002**, *41* (25), 6518.

(8) Chen, Z.; Yan, Y.; Elnashaie, S. S. E. H. Modeling and Optimization of a Novel Membrane Reformer for Higher Hydrocarbons. *AIChE J.* **2003**, *49* (5), 1250.

(9) Uemiya, S. State-of-the-art of Supported Metal Membranes for Gas Separation. *Sep. Purif. Methods* **1999**, *28* (1), 51.

(10) Kikuchi, E. Membrane Reactor Application to Hydrogen Production. *Catal. Today* **2000**, *56*, 91.

(11) Kikuchi, E.; Nemoto, Y.; Kajiwara, M.; Uemiya, S.; Kojima, T. Steam Reforming of Methane in Membrane Reactors: Comparison of Electroless Plating and CVD Membranes and Catalyst Packing Modes. *Catal. Today* **2000**, *56*, 75.

(12) Prabhu, A. K.; Liu, L. G.; Lovell, S. T.; Oyama, S. T. Modeling of the methane reforming reaction in hydrogen selective membrane reactors. *J. Membr. Sci.* **2000**, *177*, 83.

(13) Lin, Y. S. Microporous and Dense Inorganic membranes: Current Status and Perspective. *Sep. Purif. Technol.* **2001**, *25*, 39.

(14) Nam, S.; Lee, K. Hydrogen Separation by Pd Alloy Composite Membranes: Introduction of Diffusion Barrier. *J. Membr. Sci.* **2001**, *192*, 177.

(15) Silaban, A.; Harrison, D. P. High-Temperature capture of Carbon Dioxide: Characteristics of the Reversible Reaction Between CaO(s) and $CO_2$(g). *Chem. Eng. Commun.* **1995**, *137*, 177.

(16) Han, C.; Harrison, D. P. Simultaneous Shift Reaction and Carbon Dioxide Separation for the Direct Production of Hydrogen. *Chem. Eng. Sci.* **1994**, *49* (24B), 5875.

(17) Balasubramanian, B.; Lopez Ortiz, A.; Kaytakoglu, S.; Harrison, D. P. Hydrogen from Methane in a Single Step Process. *Chem. Eng. Sci.* **1999**, *54*, 3543.

(18) Han, C.; Harrison, D. P. Multicycle Performance of a Single-Step Process for $H_2$ Production. *Sep. Sci. Technol.* **1997**, *32* (1−4), 681.

(19) Hufton, J. R.; Mayorga, S.; Sircar, S. Sorption-Enhanced Reaction Process for Hydrogen Production. *AIChE J.* **1999**, *45* (2), 248.

(20) Waldron, W. E.; Hufton, J. R.; Sircar, S. Production of Hydrogen by Cyclic Sorption Enhanced Reaction Process. *AIChE J.* **2001**, *47* (6), 1477.

(21) Abanades, J. C. The Maximum Capture Efficiency of $CO_2$ using a Carbonation/Calcination Cycle of CaO/$CaCO_3$. *Chem. Eng. J.* **2002**, *90*, 303.

(22) Trimm, D. L. The Formation and Removal of Coke from Nickel Catalyst. *Catal. Rev.—Sci. Eng.* **1977**, *16* (2), 155.

(23) Bartholomew, C. H. Carbon Deposition in Steam Reforming and Methanation. *Catal. Rev.—Sci. Eng.* **1982**, *24* (1), 67.

(24) Xu, J.; Froment, G. F. Methane Steam Reforming, Methanation and Water Gas Shift—I. Intrinsic Kinetics. *AIChE. J.* **1989**, *35*, 88.

(25) Elnashaie, S. S. E. H.; Adris, A. M.; Al-Ubaid, A. S.; Soliman, M. A. On the Non-Monotonic Behavior of Methane Steam Reforming Kinetics. *Chem. Eng. Sci.* **1990**, *45* (2), 491.

(26) Bhatia, S. K.; Perlmutter, D. D. Effect of the Product Layer on the Kinetics of the $CO_2$−Lime Reaction. *AIChE J.* **1983**, *29* (1), 79.

(27) Mess, D.; Sarofim, A.; Longwell, J. P. Product layer Diffusion during the reaction of Calcium Oxide with Carbon Dioxide. *Energy Fuels* **1999**, *13*, 999.

(28) Patience, G. S.; Chaouki, J.; Berruti, F.; Wong, R. Scaling Considerations for Circulating Fluidized Bed Risers. *Powder Technol.* **1992**, *72*, 31.

(29) Haider, A.; Levenspiel, O. Drag Coefficient and Terminal Velocity of Spherical and Nonspherical Particles. *Powder Technol.* **1989**, *58*, 63.

(30) Kunii, D.; Levenspiel, O. Circulating Fluidized-Bed Reactors. *Chem. Eng. Sci.* **1997**, *52*, 2471.

*Received for review* June 30, 2003
*Revised manuscript received* October 11, 2003
*Accepted* October 20, 2003

IE030524I